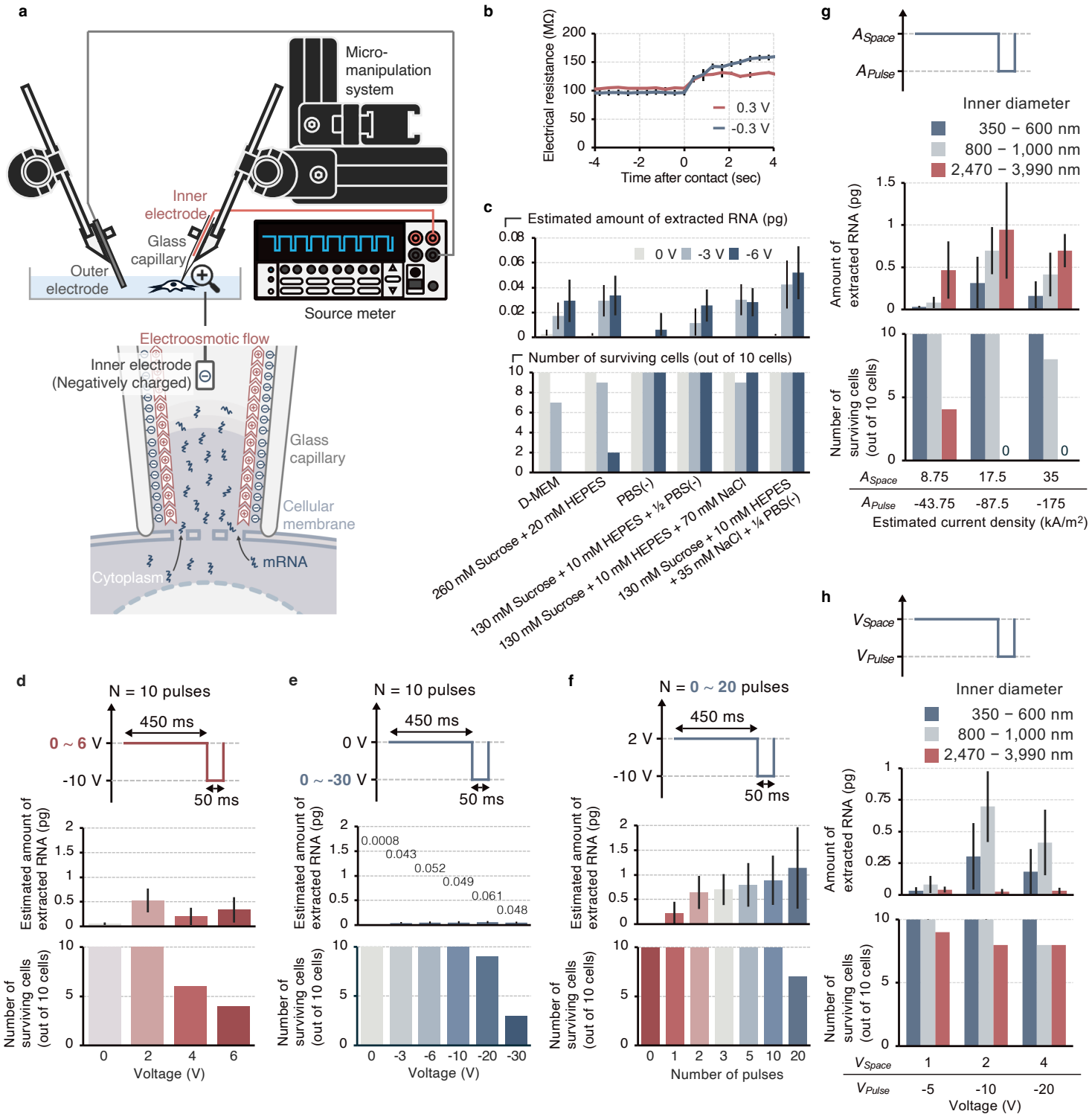

Supplementary Fig. 1. (**a**) (Upper) Setup for the nanoelectrokinetic sampling method. A glass capillary with nano-scale pore is carefully placed on the cell membrane by the micro-manipulation system. The tip of the capillary is filled with a sucrose solution. An electrode connected to the source meter is immersed in the inner solution of capillary and the other in the medium. The contact between the capillary and the cellular membrane is monitored by an increase in the electrical resistance. After the contact, a voltage adjusted for sampling is applied for reversible electroporation. Electroosmotic flow aspirates subcellular biopsies through the pores into the capillary. (**b**) Changes in electrical resistance before and after the contact of capillary onto cellular membrane. (**c-f**) qPCR-based measurement of extracted mRNA (n = 5) and count for survival cells after sampling (n = 10) in various conditions, buffers (c), the applied voltage for electroporation (d), the magnitude of the voltage for extraction (e), the number of applications (f). (**g, h**) Examination of the inner diameter of capillary on the basis of current (g) and voltage (h). Error bars s.d..

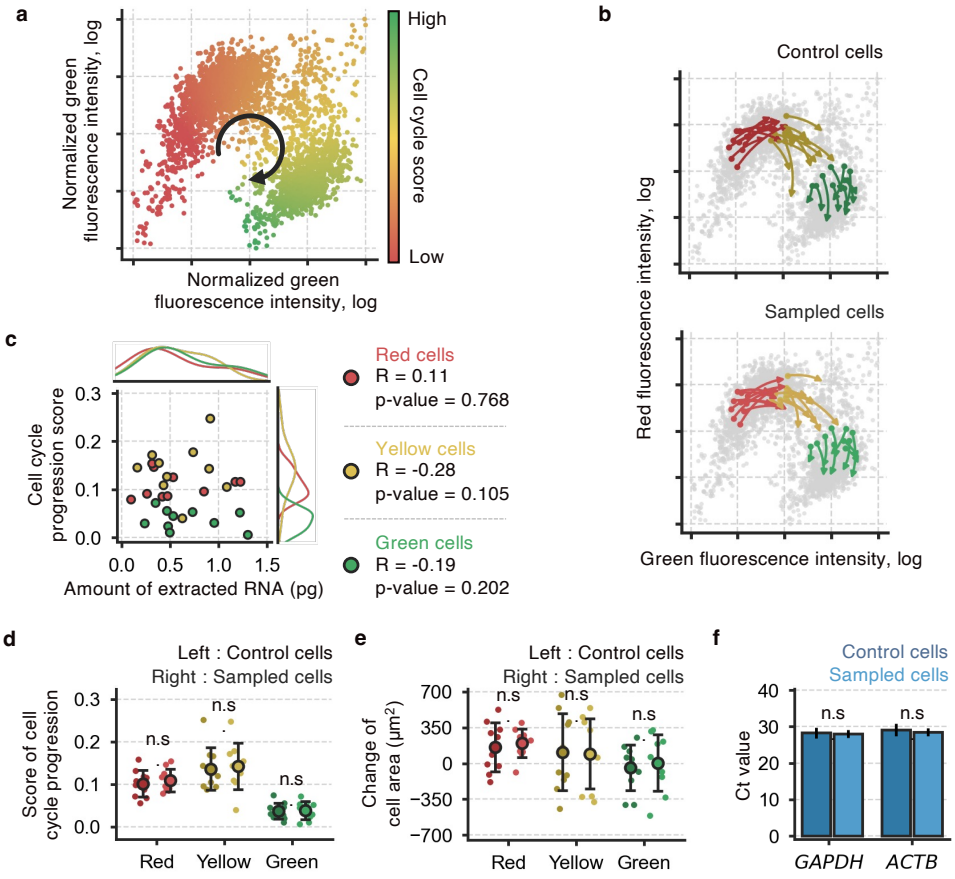

Supplementary Fig. 2. (**a**) Evaluation of cell cycle score based on Fucci intensity of each HeLa/Fucci(SA)2 cell. (**b**) Transitions of Fucci pattern in each cell before sampling and after 2.5 h. Arrows show the 2.5 h transition. Control cells are nearest neighbors of the sampled cells in the space of Fucci fluorescence intensity. The colors of arrows indicate Fucci fluorescence intensities in pre-sampling cells. (**c**) Relation between post-sampling progression of cell cycle and amount of extracted RNA in each cell. Score of cell cycle progression is the difference of cell cycle scores before and after sampling. *P* value was estimated with a two-tailed *t* test. n=10. (**d**) Comparation of score of cell cycle progression between sampled cells and control cells. *P* value was estimated with a two-tailed *t* test. n.s. p-value > 0.05. n=10. (**e**) Comparation of change in cell area before and after sampling. *P* value was estimated with a two-tailed *t* test. n.s. p-value > 0.05. n=10. (**f**) Ct values of housekeeping genes, *GAPDH* and *ACTB*, in red fluorescent cells 2.5 h after sampling and control cells. *P* value was estimated with a two-tailed *t* test. n.s. p-value > 0.05. n = 5. Error bars s.d..

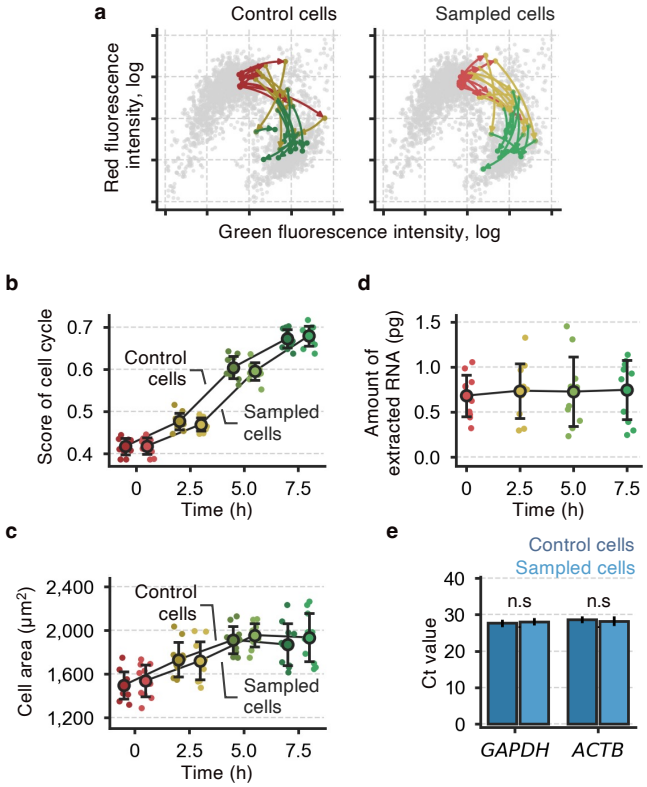

Supplementary Fig. 3. (**a**) Transitions of Fucci pattern in cells during repeated sampling every 2.5 h four times and control cells. The colors of arrows indicate cell cycle phase during steps of imaging. (**b**) Cell cycle scores in cells shown in (a). n = 10. (**c**) Amount of extracted RNA at each time point. n = 10. (**d**) Time-series of cell area. n = 10. (**e**) Ct values of housekeeping genes, *GAPDH* and *ACTB*, comparing between sampled cells and control cells. n = 5. *P* value was estimated with a two-tailed *t* test. n.s. p-value > 0.05. Error bars s.d..

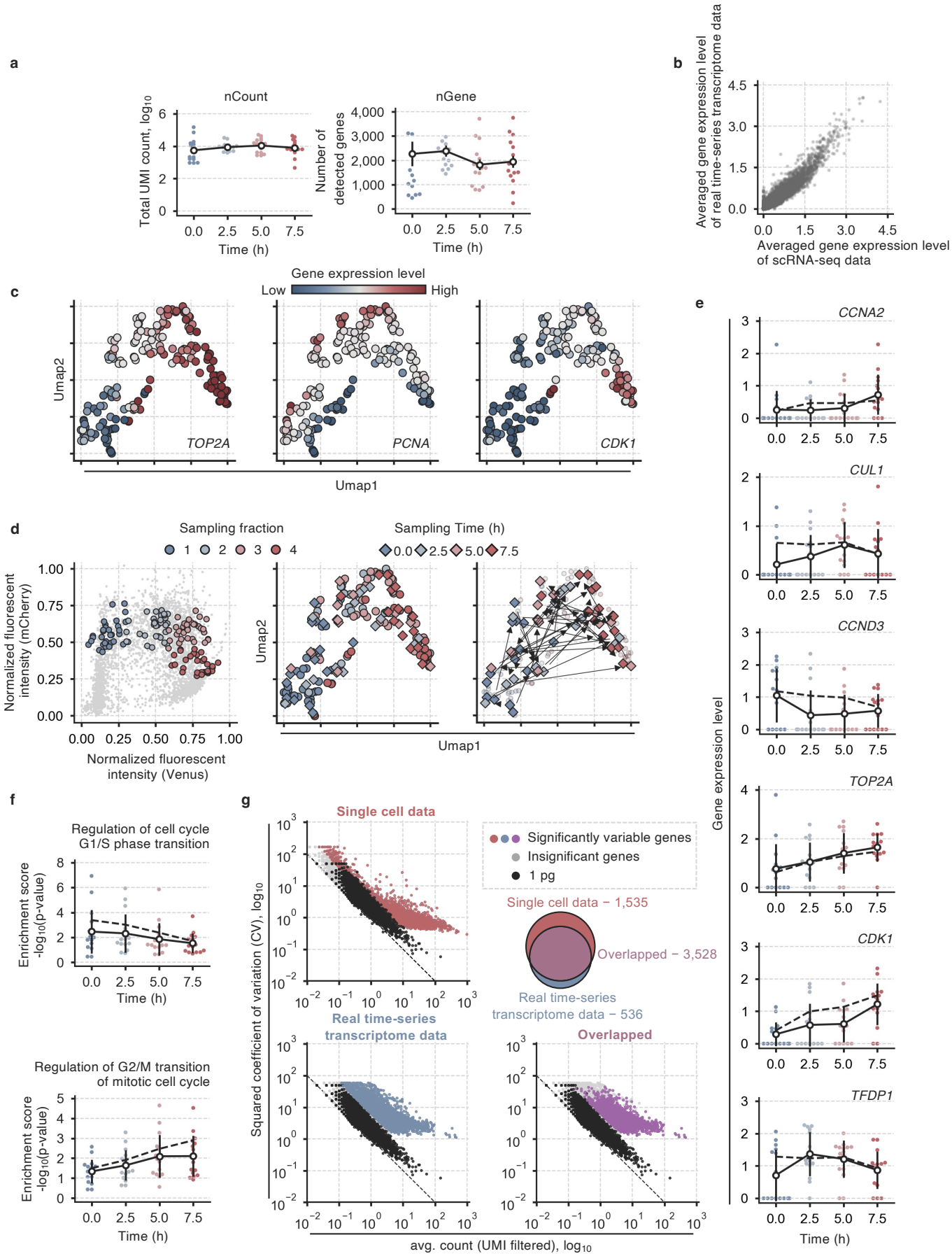
a
nCount
nGene
Total UMI count, log10
Number of detected genes
Time (h)
b
Averaged gene expression level of real time-series transcriptome data
Averaged gene expression level of scRNA-seq data
c
Gene expression level
Low
High
Umap2
Umap1
TOP2A
PCNA
CDK1
d
Sampling fraction
Sampling Time (h)
Normalized fluorescent intensity (mCherry)
Normalized fluorescent intensity (Venus)
e
CCNA2
CUL1
CCND3
TOP2A
CDK1
TFDP1
Gene expression level
Time (h)
f
Regulation of cell cycle G1/S phase transition
Regulation of G2/M transition of mitotic cell cycle
Enrichment score -log10(p-value)
g
Single cell data
Significantly variable genes
Insignificant genes
1 pg
Single cell data − 1,535
Overlapped − 3,528
Real time-series transcriptome data − 536
Real time-series transcriptome data
Overlapped
Squared coefficient of variation (CV), log10
avg. count (UMI filtered), log10

Supplementary Fig. 4. (**a**) Temporal changes in total UMI counts and number of detected genes in real time-series data. (**b**) Correlation between the gene expression profiles of pseudo bulk created by accumulating real time-series transcriptome data and that created by accumulating scRNA-seq data. Pearson's r = 0.959. (**c**) A continuum trajectory of batch collected real time-series transcriptome data and scRNA-seq data in UMAP space overlaid by expression levels of cell cycle markers. (**d**) (Left) Corrected fluorescent signals of each cell paired with scRNA-seq data and live-cell transcriptome data. Batch correction of fluorescence intensities was performed by histogram matching of both green and red intensities in two datasets. (Middle) Visualization of sampling fraction for FACS and sampling time in real time-series data on the trajectory in UMAP space. (Right) Cell-by-cell transitions of transcriptome recorded in real time-series transcriptome data. Arrows indicate the transition in 2.5 hours sampling interval. (**e**) Expression pattern of cell cycle markers in real time-series data shown as solid lines. Doted lines show averages of the expression level in each sampling fraction of scRNA-seq data arranged from left to right: 1, 2, 3, 4. (**f**) The temporal patterns of enrichment scores, based on GO term analysis with real-time series data, are depicted as solid lines. Dotted lines represent the enrichment scores of each sampling fraction of scRNA-seq data arranged from left to right: 1, 2, 3, 4. (**g**) Coefficient of variation vs. mean plots (CV-mean plots) of scRNA-seq data (Upper left) and real time-series transcriptome data (Lower left). 1 pg bulk RNA control (black); significantly variable genes than control (red and blue). (Upper right) Venn diagram of significantly variable genes from the real time-series transcriptome and scRNA-seq data. (Lower right) Overlapped genes in the Venn diagram on CV-mean plot of real time-series transcriptome data. The dotted line indicates Poisson noise. Error bars s.d..

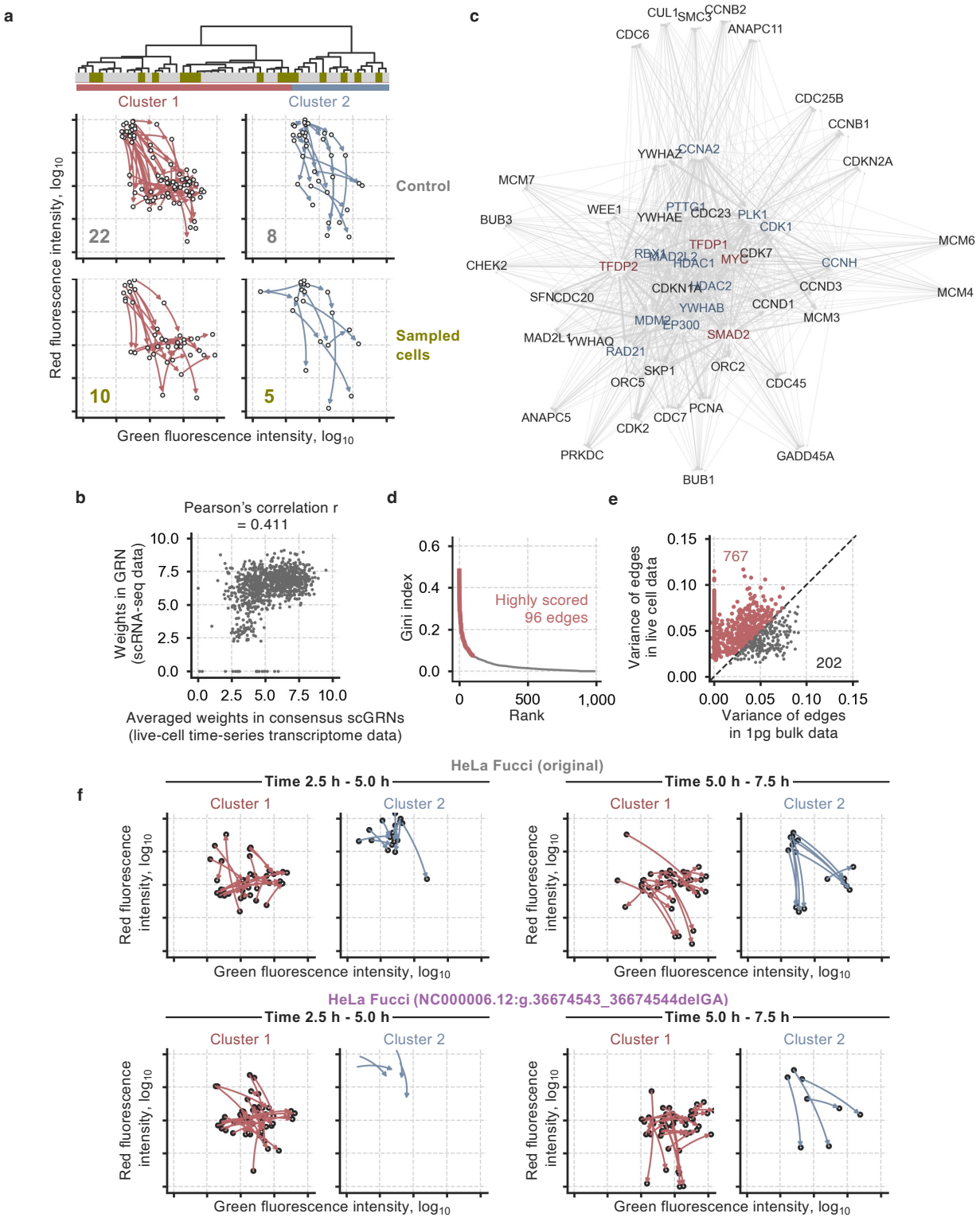

Supplementary Fig. 5. (**a**) Patterns of cell cycle progression in repeatedly sampled HeLa/Fucci cells and unsampled cells (control). (Upper) hierarchical clustering showed the major two clusters with the distinct cell-cycle patterns of control cells indicated by light gray and sampled cells indicated by yellow. Bottom panel showed temporal changes of Fucci fluorescence signals by each cluster (cluster 1 or 2) and condition (control or sampled). Fisher's exact test revealed an insignificant p-value of 0.7324 for the comparison of control vs sampled cells. (**b**) Correlation between the edge weights in consensus scGRN and GRN inferred from an ensemble of scRNA-seq. (**c**) The consensus scGRN with gene symbols shown in Fig. 1c. (**d**) Elbow plot showing rank-ordered genes by Gini index. (**e**) Comparison of variance of edge weights between consensus scGRN and consensus scGRNs predicted from 1pg bulk RNA-seq datasets. The 1pg bulk RNA-seq dataset comprises five RNA-seq data for every four time points assembled along cell cycle. Edges with higher variance in scGRNs are shown in red and those with lower variance in gray. The number of edges is shown in the panel. (**f**) Patterns of cell cycle progression observed in the cells shown in Fig. 2d over the subsequent five hours.

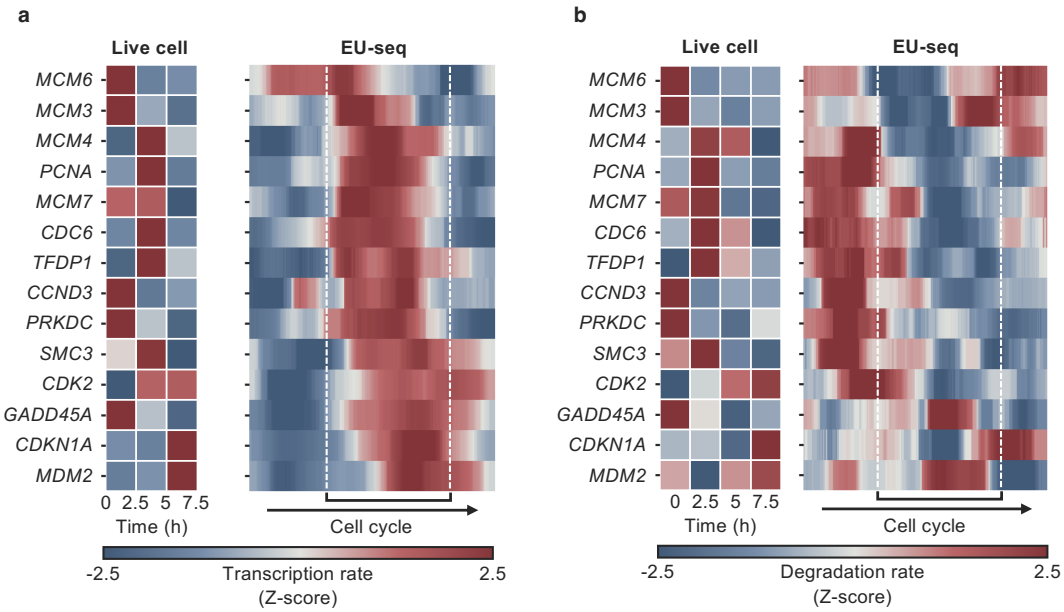

Supplementary Fig. 6. Transcription (**a**) and degradation (**b**) rates of cell cycle related genes estimated from live-cell time-series transcriptome data (left) and from scEU-seq data (right).[17] The area enclosed by the white dot lines indicate the period during which we performed sampling.

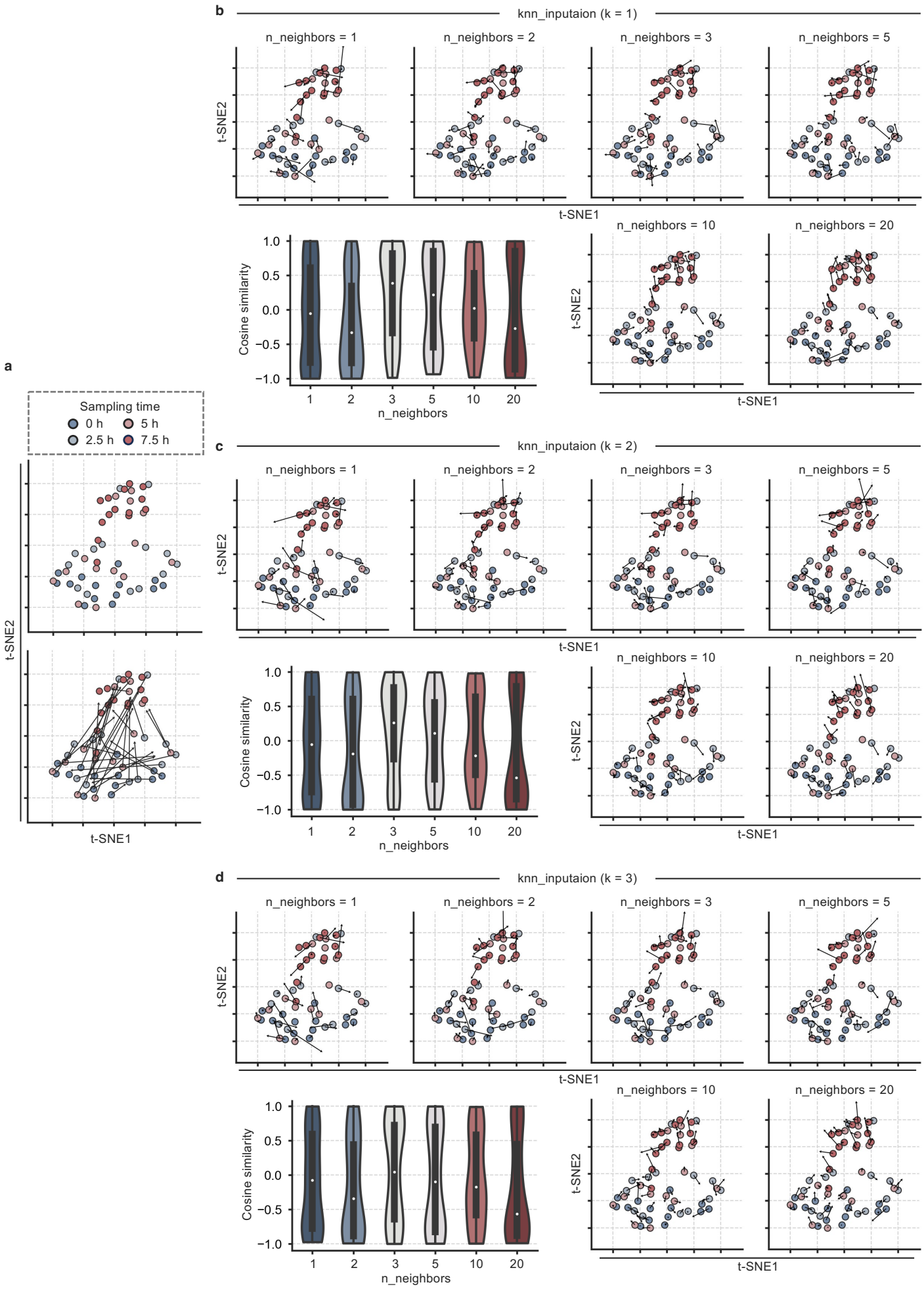
a
Sampling time
0 h
2.5 h
5 h
7.5 h
t-SNE2
t-SNE1
b
knn_inputaion (k = 1)
c
knn_inputaion (k = 2)
d
knn_inputaion (k = 3)
n_neighbors = 1
n_neighbors = 2
n_neighbors = 3
n_neighbors = 5
n_neighbors = 10
n_neighbors = 20
Cosine similarity
1.0
0.5
0.0
−0.5
−1.0
1
2
3
5
10
20
n_neighbors

Supplementary Fig. 7. (**a**) t-SNE plot displaying data from each timepoint of the live-cell time-series transcriptome data. Arrows in the lower panel represent transitions of individual cells in 2.5 h on the t-SNE plot. (**b-d**) RNA velocity estimated by velocyto under various parameters is shown by arrows in t-SNE plots. At the bottom left of each figure, the cosine similarity between the RNA velocity evaluated under each n_neighbors parameter and the real velocity shown in (a) is indicated.

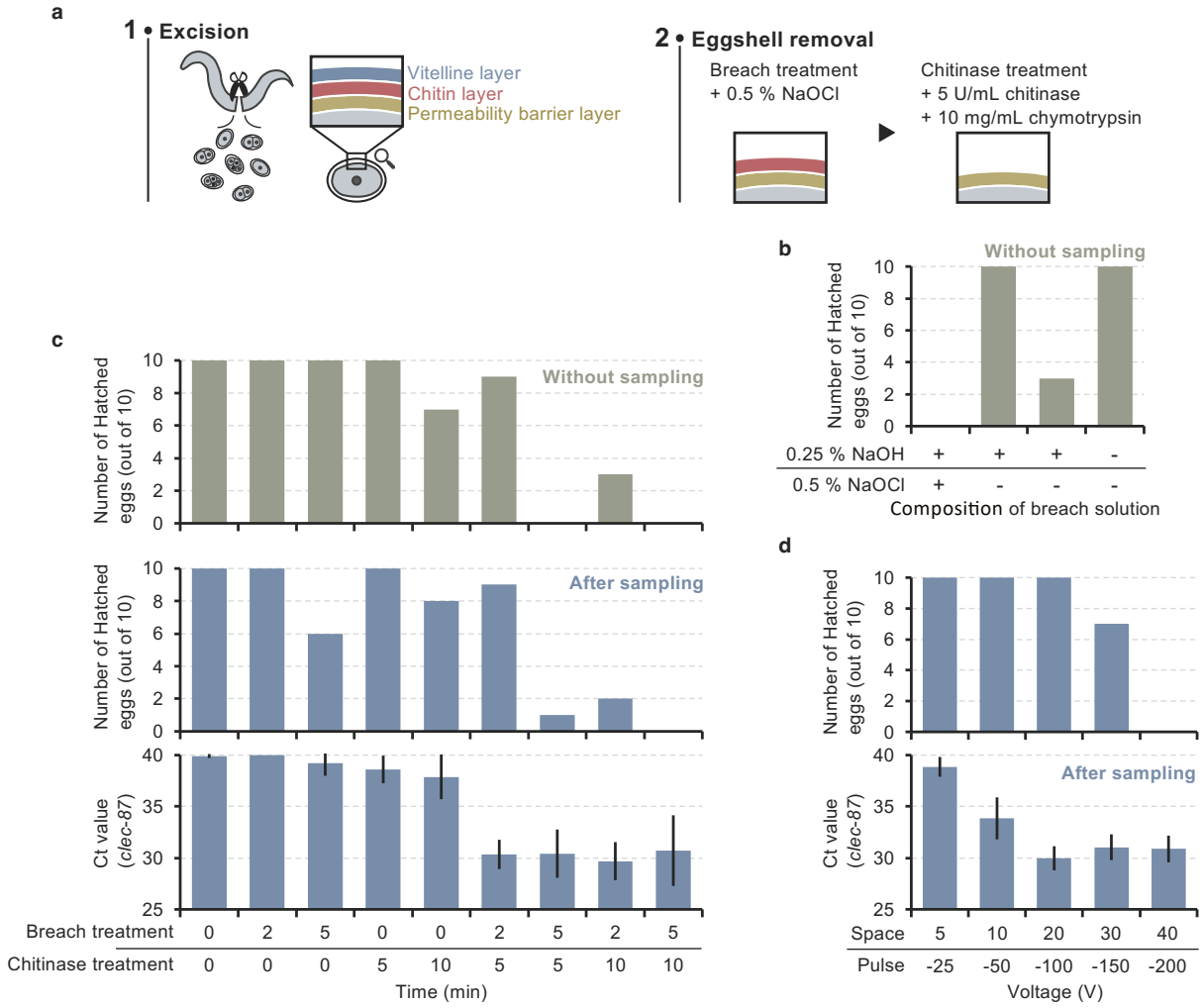

Supplementary Fig. 8. (**a**) Procedure for preparation of nematode zygotes for live-organism sampling. (**b**) Hatchability rates of wild-type (N2) zygotes following eggshell removal using bleach solutions of different compositions. (**c**) (Top) Comparison of hatchability among various treatment durations of bleach and chitinase solutions. (Middle) Hatchability of eggshell removed embryos after repeated samplings. (Bottom) Relative amount of extracted RNA from zygotes with different treatment durations. (**d**) Hatchability and Ct values under various application conditions for RNA extraction. n = 5 for qPCR. Error bars s.d..

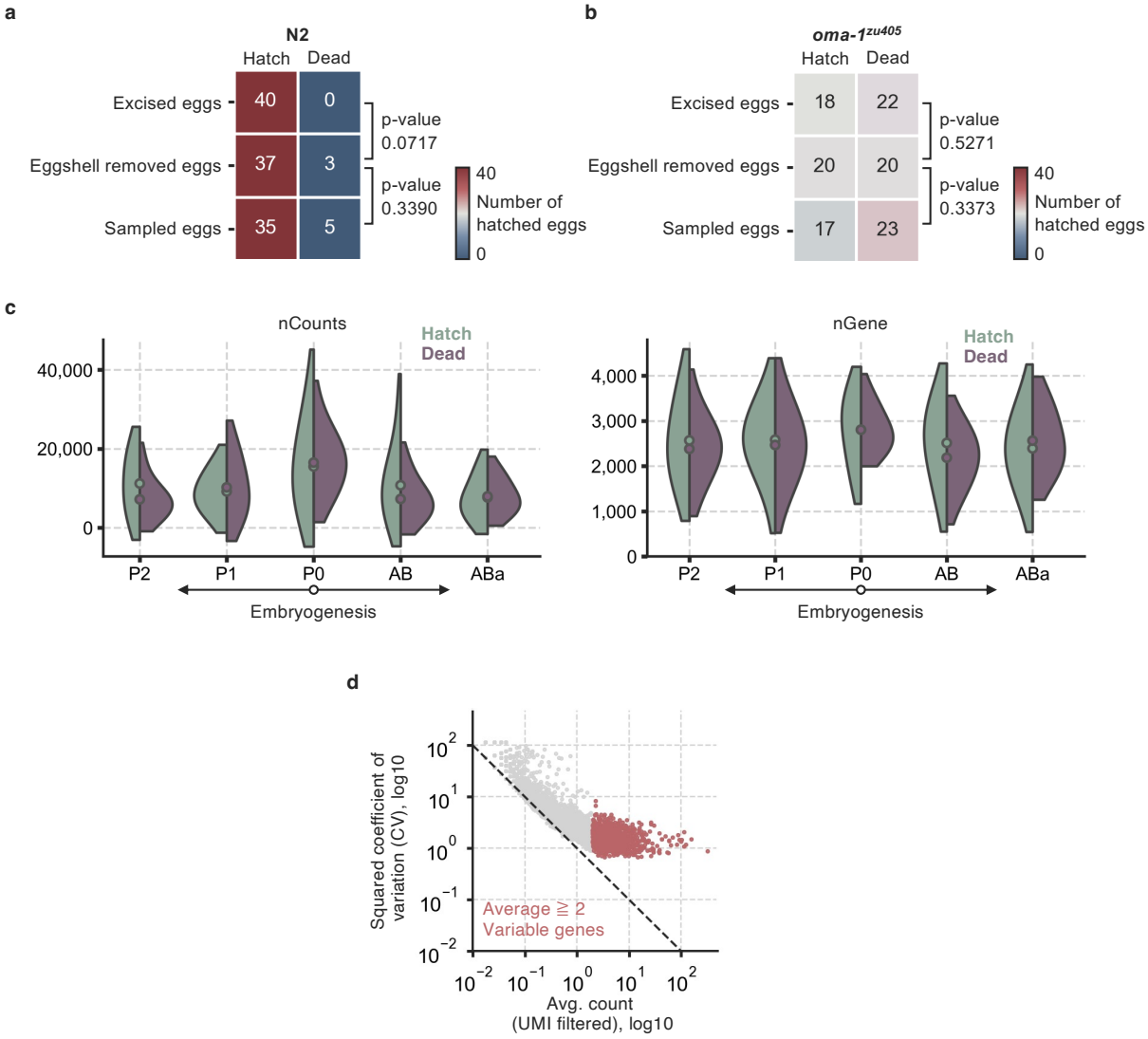

Supplementary Fig. 9. (**a, b**) Hatchability of freshly excised zygotes, zygotes with removed eggshells, and repeatedly sampled are presented for wild-type (N2) (a) and *oma-1*^{zu405} (b). The hatchability was assessed for 40 embryos per condition. *P* values were calculated using a chi-squared test. (**c**) Total UMI counts and the number of detected genes in hatching embryos and mortal embryos are depicted. (**d**) CV-mean plot for live-organism transcriptome data. The dotted line indicates Poisson noise. Genes with two or more average UMI counts were selected as variable genes and highlighted in red.

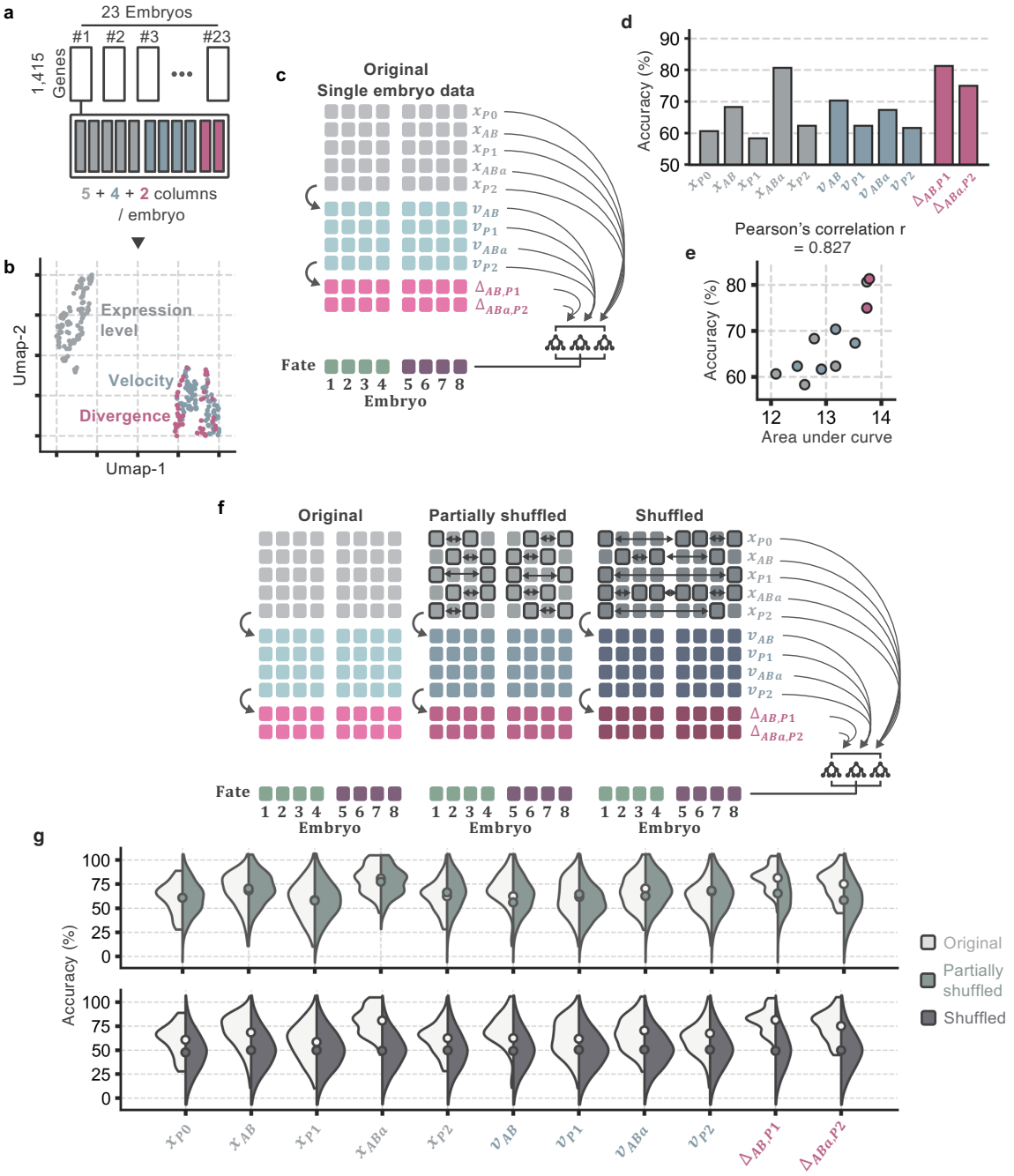

Supplementary Fig. 10. (**a**) The single-embryo data concatenated horizontally with each feature. (**b**) UMAP visualization of the single-embryo data shown in (a). (**c**) Cross-validation based on classification analysis was conducted for each feature type of single-embryo data to determine the prediction accuracy of fate. (**d**) The prediction accuracy of fate for each feature type. (**e**) Correlation between the prediction accuracy and the area under the curve shown in Fig. 3e. The color of points indicates feature types. (**f,g**) Comparison of fate prediction accuracy of each feature type between original and shuffled single-embryo data.

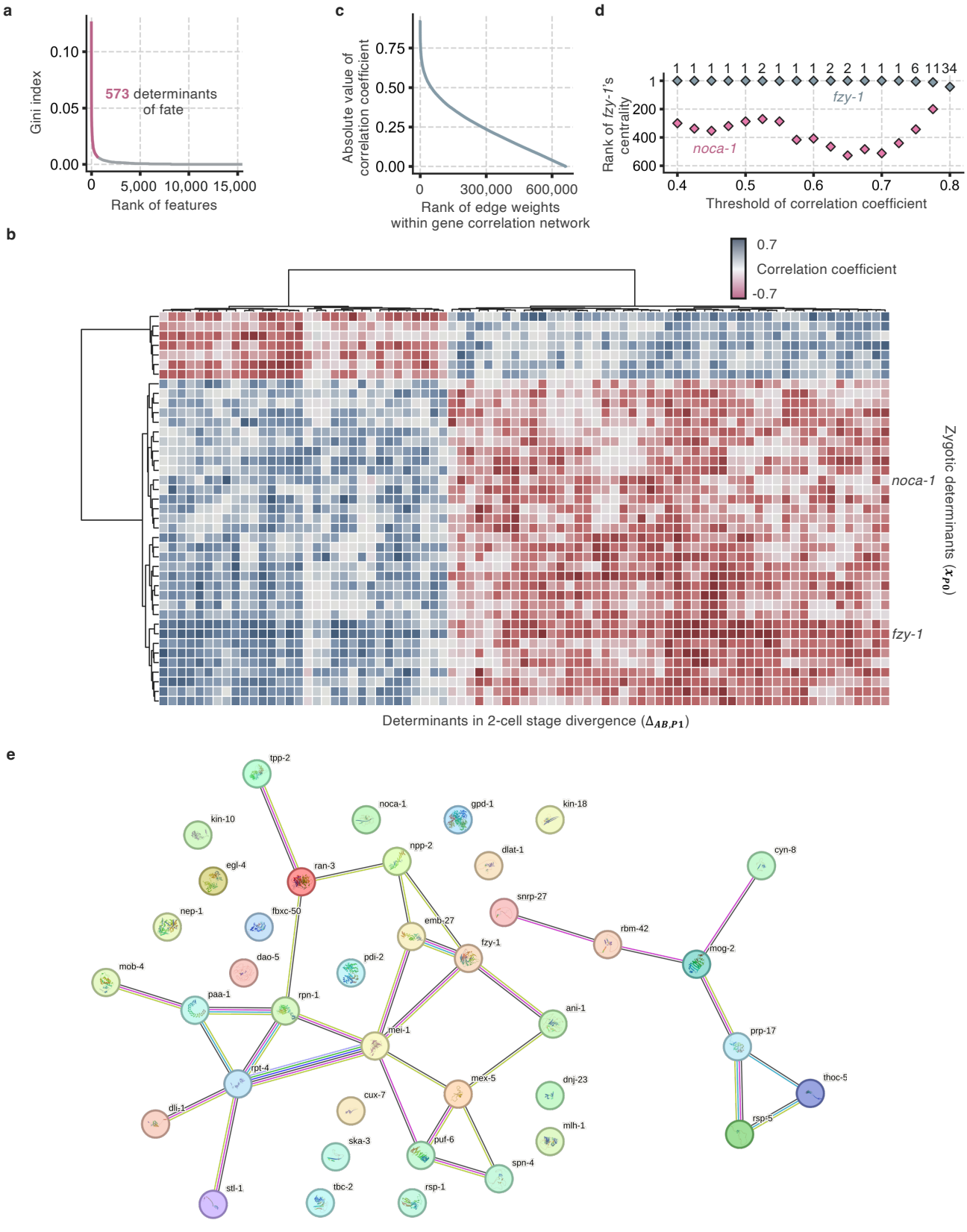

Supplementary Fig. 11. (**a**) Elbow plot showing rank-ordered features by Gini index. High-scoring features are selected as determinants of fate. (**b**) Correlation matrix showing correlation between zygotic determinants and determinants of 2-cell stage divergence. (**c**) Elbow plot showing rank-ordered correlations between the determinants by Spearman's ρ. (**d**) The rank of closeness centrality of *fzy-1* and *noca-1* in the gene correlation network based on various thresholds of correlation coefficient. In a gene correlation network with a correlation coefficient threshold set to 0.8, *noca-1* had no edges. (**e**) Protein–protein association networks consisted of zygotic determinants obtained from STRING database.